ELECTRONIC STRUCTURE
OF DOPED La–Mn–O PEROVSKITES

M. Demeter[a,*], M. Neumann[a], V.R. Galakhov[b], N.A. Ovechkina[b],
E.Z. Kurmaev[b] and N.I. Labachevskaya[c]

[a]University of Osnabrück, Faculty of Physics
Barbarastr. 7, 49069 Osnabrück, Germany
[b]Institute of Metal Physics, Russian Academy of Sciences – Ural Division
620219 Yekaterinburg GSP-170, Russia
[c]Institute of Chemistry of Solids, Russian Academy of Sciences – Ural Division
620219 Yekaterinburg GSP -145, Russia

The electronic structure of the doped perovskite manganese oxides $La_{1-x}Sr_xMnO_3$ and $La_{1-x}Ba_xMnO_3$ has been investigated by X-ray photoelectron and X-ray emission spectroscopy. By comparing the O K_α and Mn L_α X-ray emission spectra with the valence band X-ray photoelectron spectra we could localize the Mn $3d$ and O $2p$ states into the valence band. Our data are compared with previous band structure calculations. The value of the Mn $3s$ splitting does not change with Sr-doping in the concentration region from $x = 0.0$ till $x = 0.3$. This shows that the doping holes have mainly oxygen p character. The large value of the splitting indicates that the $3d$ electrons are in the high-spin state.

PACS numbers: 71.70.Gm, 79.70.+q

1. Introduction

Nowadays great interest exists in manganese perovskite oxides due to the discovery of the colossal magnetoresistance (CMR) effect [1]. The parent compound $LaMnO_3$ is an A-type antiferromagnetic (AFM) ($T_N = 140$ K) insulator with a distorted perovskite structure. The manganese ions are Mn^{3+} ($3d^4$) having three electrons in the t_{2g} band and one in the e_g band. When this compound is doped with divalent alkaline-earth cations A^{2+} (Sr, Ba), a charge redistribution from Mn^{3+} to Mn^{4+} occurs. In a certain range of doping $(0.2 \div 0.5)$ these compounds show simultaneously ferromagnetism and metallic behaviour. This effect has been explained by Zenner in the double-exchange model [2]. According to this, the conduction is achieved through the hopping of an electron in the e_g state of the Mn^{3+} ions into the unoccupied e_g band of the Mn^{4+} ions. Later it has been shown

---

*corresponding author; e-mail: mdemeter@uos.de

that the electron–phonon interaction also plays a very important role [3]. The microscopic origin of the strong electron–phonon coupling is the large Jahn–Teller effect which occurs for d^{4+} ions in an octahedral environment [4].

The electronic and magnetic diagram of $La_{1-x}Sr_xMnO_3$ has been established from electrical and magnetic measurements. Curie temperatures of 145 K, 309 K, and 369 K for $x = 0.1, 0.2, 0.3$ were also determined [5]. For $x < 0.1$ the system is a canted AFM insulator and for $0.1 < x < 0.17$ it is FM insulator. For $x = 0.175$ at room temperature there is also a structural transition from orthorhombic to rhombohedral. For $x > 0.2$ a transition from FM insulator to FM metal takes place. The crystal structure of $La_{1-x}Ba_xMnO_3$ changes from orthorhombic through rhombohedral to cubic ($x > 0.35$) with increasing concentration. The Curie temperatures of $La_{1-x}Sr_xMnO_3$, where $x = 0.1, 0.2, 0.3$ are 145 K, 309 K, and 369 K, respectively.

X-ray photoelectron and X-ray emission spectroscopies (XPS, XES) are known as powerful tools to investigate the electronic structure of perovskites and the changes with carriers doping. In this paper we present new results of XPS and XES studies of the single crystals of $La_{1-x}Sr_xMnO_3$ ($x < 0.3$) and $La_{0.8}Ba_{0.2}MnO_3$. Our experimental spectra are compared with the previous band structure calculations [6].

2. Experimental

Single crystals of $La_{0.8}Ba_{0.2}MnO_3$, $(La_{0.9}Sr_{0.1})_{0.9}MnO_3$, $La_{0.8}Sr_{0.2}MnO_3$, and $La_{0.7}Sr_{0.3}MnO_3$ were grown by the floating-zone method using the radiation heating of the zone by a xenon lamp at the Moscow Institute of Steel and Alloys by Ya.M. Mukovskii.

The X-ray photoelectron spectra were recorded with an ESCA spectrometer from Physical Electronics (PHI∼5600∼ci) using monochromatic Al K_α radiation. All samples were measured after breaking in a high vacuum (10^{-9} torr). All spectra were recorded at room temperature. They were calibrated using an Au-foil (E_B ($4f_{7/2}$) $= 84.0$ eV). The energy resolution as determined at the Fermi level of the Au-foil was ~ 0.4 eV.

The Mn L_α ($3d4s \rightarrow 2p_{3/2}$ transitions) and O K_α ($2p \rightarrow 1s$ transitions) X-ray emission spectra were measured on the RSM-500-type X-ray vacuum spectrometer with a diffraction grating ($N = 600$ lines/mm, $R = 6$ m) and electron excitation. The spectra were recorded in the first order of reflection by a secondary electron multiplier with a CsI photocathode. The energy resolution was 0.4 eV. The X-ray tube was operated at $V = 4.0$ keV and 0.25 mA.

3. Results and discussions

In Fig. 1a the valence band spectra of $La_{0.7}Sr_{0.3}MnO_3$, $La_{0.8}Sr_{0.2}MnO_3$, and $(La_{0.9}Sr_{0.1})_{0.9}MnO_3$ are presented. They exhibit a structured wide band followed by a lower binding energy tail close to the Fermi level. The peaks at 6 eV and 2.5–4 eV correspond to the O $2p$ states hybridized with Mn t_{2g} states. The low

intensity feature close to the Fermi level that is centred at ~ 0.7 eV is due to the emission from the e_g states. The most prominent peak at 6 eV below the Fermi level does not change with x. The intensity of the La $5p$ peak, located at ~ 17 eV decreases with Sr doping, whereas Sr $4p_{3/2}$ peak at ~ 19 eV is increasing with x. The peak due to O $2s$ states is located at 21.5 eV. Similar studies on La$_{0.84}$Sr$_{0.16}$MnO$_3$ single crystal [7] and polycrystalline samples ($x = 0.0 \div 0.9$) [8] were reported.
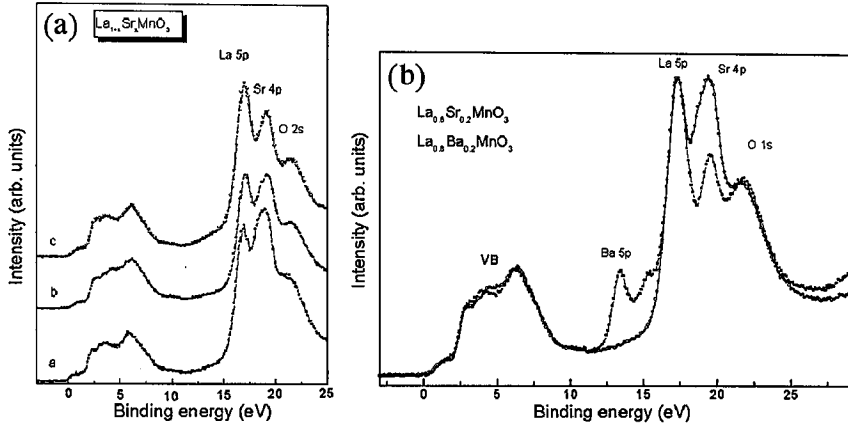

Fig. 1. (a) XPS valence band spectra of the single crystals La$_{0.7}$Sr$_{0.3}$MnO$_3$ — a, La$_{0.8}$Sr$_{0.2}$MnO$_3$ — b and (La$_{0.9}$Sr$_{0.1}$)$_{0.9}$MnO$_3$ — c; the inset shows a comparison between a — up triangle and c — line from –2 to 10 eV. (b) Comparison of the XPS valence band spectra of La$_{0.8}$A$_{0.2}$MnO$_3$ (A=Sr, Ba).

In Fig. 1b we present a comparison of the XPS valence band spectra of the single crystals La$_{0.8}$(Sr,Ba)$_{0.2}$MnO. They exhibit similar features, a wide band and a low structure close to the Fermi level. There is a difference in the feature located at about 5 eV where O $2p$ contribution dominates. For Ba doped compound ($x = 0.35$) it was found that the feature corresponding to this energetic value is not enhanced at a photon energy of 52 eV (the Mn $3p$ resonance edge) indicating that it has a very little Mn $3d$ character [9]. We assign the structure close to the Fermi level to e_g states, whereas the states at 2.9 eV are assigned to t_{2g} states [6, 9]. The next feature at ~ 4 eV is due to O $2p$ states hybridised with Mn t_{2g} states. The highest peak at ~ 6 eV is the same as in the similar Sr-doped compound. Linear muffin-tin orbital (LMTO) band structure calculations performed on the La$_{1-x}$Ba$_x$MnO system [10] have shown that for $x = 0.2$ the contribution to the total density of states (DOS) at the Fermi level comes mainly from e_g states, whereas for $x = 0.4$, in the half-metallic regime ($x > 0.33$) the density of states at E_F is due solely to e_g electrons. In the Ba-doped sample, the peak located at 13.4 eV is due to Ba $5p$ states. The feature at binding energies higher than 25 eV in the Ba-doped sample is given by the Ba $5s$ peak contribution (not shown here).

In Fig. 2 XPS valence band together with XES Mn L_α and O K_α spectra are shown for LaMnO$_3$ and Sr(Ba)-doped samples ($x = 0.2$). Mn L_α X-ray emission

arises from the $3d4s \rightarrow 2p_{3/2}$ electronic transition and reflects the Mn $3d$ distribution in the valence band. O K_α X-ray emission corresponds to the $2p \rightarrow 1s$ transition and reveals the O $2p$ partial density of states. The XES Mn L_α and O K_α spectra were brought to the binding energy scale by using the Mn $2p_{3/2}$ and O $1s$ binding energies, respectively. The Mn L_α and O K_α XES spectra are localized in the same energy area, which indicates a strong Mn $3d$ – O $2p$ hybridization. In the O K_α spectrum, the maximum at ~ 3.5 eV corresponds to the antibonding $pd\pi$ states and the shoulder at 6 eV reflects the bonding $pd\sigma$ states. Our experimental results are in good agreement with local spin-density approximation (LSDA) calculations [6].
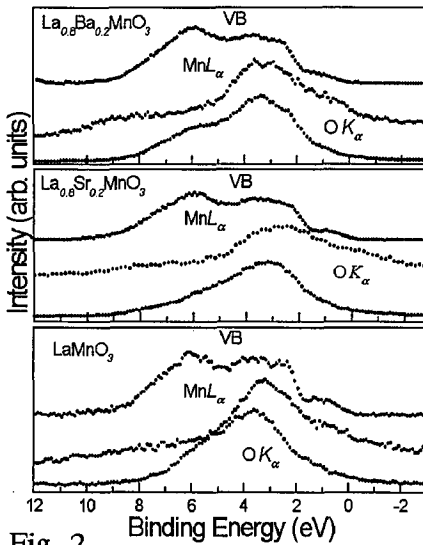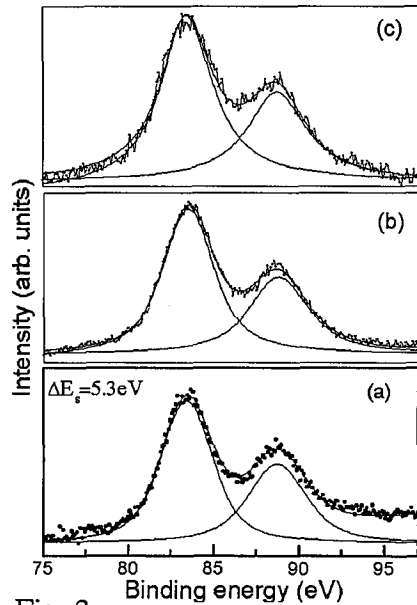

Fig. 2.   XPS and XES spectra of $LaMnO_3$, $La_{0.8}Sr_{0.2}MnO_3$, and $La_{0.8}Ba_{0.2}MnO_3$.
Fig. 3.   XPS Mn $3s$ splitting of the single crystals of $La_{0.7}Sr_{0.3}MnO_3$ (a), $La_{0.8}Sr_{0.2}MnO_3$ (b), and $(La_{0.9}Sr_{0.1})_{0.9}MnO_3$ (c).

The $3s$ exchange splitting in transition metal compounds is due to the exchange interaction between the $3s$ core hole created in a XPS process and $3d$ electrons. The magnitude of the Mn $3s$ splitting (ΔE_s) depends on the valence state of the Mn ions. In Fig. 3 the Mn $3s$ XPS spectra of $(La_{0.9}Sr_{0.1})_{0.9}MnO_3$, $La_{0.8}Sr_{0.2}MnO_3$, and $La_{0.7}Sr_{0.3}MnO_3$ single crystals are presented. The highest peak is located at ~ 83.5 eV. In Ref. [8] it has been reported that the Mn $3s$ splitting of polycrystalline $La_{1-x}Sr_xMnO_3$ ($x = 0.0 \div 0.9$) monotonically decreases with x. However, our spectra on single crystals samples show that the value of the Mn $3s$ splitting (5.3 eV) does not change with Sr doping from $x = 0.0$ to $x = 0.3$. This indicates that the doped holes have mainly oxygen p character. The large value of the splitting is consistent with the high-spin configurations.

4. Conclusions

We have presented new XPS and XES results on manganese doped perovskites, single crystals. The same $3s$ splitting of the Sr-doped samples with $x < 0.3$ indicates the oxygen $2p$ character of the doped holes. The large value of the splitting shows that the Mn $3d$ electrons are in the high spin state. The Mn L_α and O K_α XES spectra are localised in the same energy area indicating strong Mn $3d$ – O $2p$ hybridisation. Our data are in good agreement with the previous LSDA results.

Acknowledgments

References

[1] A.P. Ramirez, *J. Phys., Condens. Matter* **9**, 8171 (1997); J.M.D. Coey, M. Viret, S. von Molnár, *Adv. Phys.* **48**, 167 (1999).

[2] C. Zener, *Phys. Rev.* **82**, 403 (1951); J. Goodenough, *Phys. Rev.* **100**, 564 (1955).

[3] A.J. Millis, P.B. Littlewood, B.I. Shraiman, *Phys. Rev. Lett.* **74**, 5144 (1995); A.J. Millis, B.I. Shraiman, R. Mueller, *Phys. Rev. Lett.* **77**, 175 (1996).

[4] J.R. Fletcher, K.W.H. Stephens, *J. Phys. C, Solid State Phys.* **2**, 444 (1969).

[5] Y. Tokura, A. Urushibara, Y. Moritomo, T. Arima, A. Asamitsu, G. Kido, N. Furukuwa, *J. Phys. Soc. Jpn.* **63**, 3931 (1994); A. Urushibara, Y. Moritomo, T. Arima, A. Asamitsu, G. Kido, Y. Tokura, *Phys. Rev. B* **51**, 14103 (1995).

[6] S. Sapathy, Z.S. Popović, F.R. Vukajlović, *Phys. Rev. Lett.* **76**, 960 (1996); D.D. Sarma, N. Shanthi, S.R. Barman, N. Hamada, H. Sawada, T. Terakura, *Phys. Rev. Lett.* **75**, 1126 (1995).

[7] Y. Kuwata, S. Suga, S. Imada, A. Sekiyama, S. Ueda, T. Iwasaki, H. Harada, T. Muro, T. Fukawa, K. Ashida, H. Yoshioka, T. Terauchi, J. Sameshima, H. Kuwahara, Y. Maritomo, Y. Tokura, *J. Electron Spectrosc. Relat. Phenom.* **88-91**, 281 (1998).

[8] T. Saitoh, A.E. Bocquet, T. Mizokawa, H. Namatame, A. Fujimori, M. Abate, Y. Takeda, M. Takano, *Phys. Rev. B* **51**, 13942 (1995).

[9] D.N. McIlroy, C. Waldfried, Jiandi Zhang, J.W. Choi, F. Foong, S.H. Liou, P.A. Dowben, *Phys. Rev. B* **54**, 17438 (1996).

[10] S.J. Youn, B.I. Min, *Phys. Rev. B* **56**, 12046 (1997).